Structural Characterizations of Rare Earth-Rich Glasses for Nuclear Waste Immobilization

I. Bardez, Daniel Caurant, J.-L. Dussossoy, P. Loiseau, C. Gervais, F. Ribot, D.R. Neuville, N. Baffier, C. Fillet

Structural Characterizations of Rare Earth-Rich Glasses for Nuclear Waste Immobilization

I. Bardez[1,2,*], D. Caurant[2], J.L. Dussossoy[1], P. Loiseau[2], C. Gervais[3], F. Ribot[3], D. R. Neuville[4], N. Baffier[2], C. Fillet[1]

[1] *Commissariat à l'Energie Atomique, Centre d'Etudes de la vallée du Rhône, DIEC/SCDV/LEBM, 30207 Bagnols-sur-Cèze, France*
[2] *Laboratoire de Chimie Appliquée de l'Etat Solide (UMR 7574), ENSCP, 11 rue Pierre et Marie Curie, 75231 Paris Cedex 05, France*
[3] *Laboratoire de Chimie de la Matière Condensée (UMR 7574), Université Pierre et Marie Curie, 4 place Jussieu, F-75252 Paris Cedex 05, France*
[4] *Laboratoire de Physique des Minéraux et des Magmas (UMR 7047-CNRS-IPGP), Université Pierre et Marie Curie, 4 place Jussieu, F-75252 Paris Cedex 05, France*
Email: isabelle-bardez@enscp.jussieu.fr

Abstract *– New nuclear glass compositions, able to immobilize highly active liquid wastes arising from high burn-up UO_2 fuel reprocessing, are being studied. Investigations are being performed on rare earth-rich glasses, known as durable matrices. After a preliminary study, a basic glass composition was selected (Glass A, wt. %) : 51.0 SiO_2 – 8.5 B_2O_3 – 12.2 Na_2O – 4.3 Al_2O_3 – 4.8 CaO – 3.2 ZrO_2 – 16.0 Nd_2O_3.*
The aim of this study is to determine the local environment of the rare earth in this glass and its evolution according to neodymium. To achieve this objective, glasses were prepared from the baseline Glass A with variable neodymium oxide amounts (from 0 to 30 wt. % Nd_2O_3). By coupling characterization methods such as EXAFS (Extended X-Ray Absorption Fine Structure) spectroscopy at the neodymium L_{III}-edge, optical absorption spectroscopy, ^{11}B, ^{27}Al MAS-NMR and Raman spectroscopy, pieces of information on the rare earth surroundings in the glass were obtained.

INTRODUCTION

New nuclear fuels with high discharge burn-up (60 000 MWj/t) have been studied for some years in France. Reprocessing of this nuclear spent fuel will generate HLW more concentrated in fission products and minor actinides than nowadays. Therefore, new glass compositions have to be developed, able to immobilise these wastes as a whole. These matrices must exhibit excellent chemical durability and higher glass transformation temperature (T_g) than those of the current borosilicate nuclear glasses.
As the actinides and lanthanides quantity is expected to be higher in the new spent fuel, our research turned towards rare earth-rich glassy matrices. Nevertheless, lanthanide aluminoborosilicate glasses (LaBS) or lanthanide aluminosilicate glasses were not chosen in this work because of their high melting temperature ($T_m \geq 1450°C$) [1,2]. Indeed, process problems could arise from the volatility of some fission products during melting and from the limited resistance of stainless steel containers during melt casting at such high temperature. After a preliminary research, an alternative glass composition was selected for this study (Glass A, wt. %) : 51.0 SiO_2 – 8.5 B_2O_3 – 12.2 Na_2O – 4.3 Al_2O_3 – 4.8 CaO – 3.2 ZrO_2 – 16.0 Nd_2O_3. In this simplified system, more than 75 wt. % of the new HLW are simulated (the other 25 wt. % did not play a fundamental role in the properties of the glass and were thus eliminated for this structural study). Relatively large quantities of sodium and boron oxides were introduced (known as fluxing agents) so as to decrease the melting temperature below 1300°C. In the following work, both environment around the rare earth in Glass A and its evolution according to Nd concentration were studied. To this end, techniques such as EXAFS spectroscopy at the L_{III}-edge of neodymium, optical absorption spectroscopy, ^{11}B, ^{27}Al MAS-NMR and Raman spectroscopy were used.

EXPERIMENTAL

From Glass A, nine samples were prepared, containing 0, 1.3, 2.5, 5, 10, 16 (= Glass A), 20, 25 and 30 wt. % Nd_2O_3. Two glasses were also prepared with lanthanum (16 and 30 wt. % La_2O_3) for MAS-NMR studies. Glasses were produced after thorough mixing of reagent grade oxide (SiO_2, H_3BO_3, Al_2O_3, ZrO_2, Nd_2O_3) and carbonate (Na_2CO_3, $CaCO_3$) powders. All glasses were melted at $T_m = 1300°C$ for 3 h in a platinum crucible (excepted for Nd25 and Nd30,

with a T_m of 1400°C because of crystallisation problems).
EXAFS analyses were performed at the LURE-DCI synchrotron source (Orsay, France), using the Nd L_{III} edge (6.2 keV). All X-ray absorption spectra were recorded in transmission mode. Data were collected under vacuum at 77 K (liquid nitrogen). EXAFS spectra were extracted with the software developed by A. Michalowicz (EXAFS_98. ppc) [3-4] and data analysis was performed with FEFF-Fit [5], following standard methods based on scattering theory. Simulations of the first and second nearest neighbors were realized by using the theoretical backscattering phase and amplitude functions calculated with the ab-initio code FEFF 8.0 [5]. Nd_2O_3, $Nd_2Si_2O_7$ and $Ca_2Nd_8(SiO_4)_6O_2$ crystalline phases were used as model compounds. Due to the large static disorder occurring around neodymium in our glasses, a cumulant analysis [6-7] of the first shell (Nd-O) was preferred. In this case, ρ(R), the radial probability distribution of atoms in the shell, is expressed as a power series of cumulants C_i (1):

$$\ln \int_0^{\infty} \frac{\rho(R) e^{\frac{-2R}{\lambda(k)}}}{R^2} e^{i2kR} dR = \sum_{n=0}^{\infty} \frac{(i2k)^n}{n!} C_n \qquad (1)$$

Third and fourth cumulants (C_3 and C_4) are thus necessary to characterise the large asymmetric distribution of distance. The third cumulant describes the asymmetry of the distribution whereas the fourth cumulant depicts symmetry deviation from Gaussian shape [6-7].
Optical transmission experiments were carried out at low temperature (T ≈ 10 K) on polished glass samples (thickness from 0.5 to 1 mm). Raman measurements were carried out on a T64000 Jobin-Yvon confocal microRaman spectrometer equipped with a CCD detector. The 514.532 nm line of a Coherent 70 Ar+ laser was used for sample excitation. This line operated between 2 W and 0.5 W.
MAS NMR spectra were recorded on a Bruker Avance 400 spectrometer at a frequency of 128.28 MHz using a Doty probe with no probe background for ^{11}B and on a Bruker DRX600 liquid spectrometer (14.1 T) operating at 156.38 MHz and equipped with a Bruker high speed MAS probe-head for ^{27}Al. Chemical shifts were either determined relative to liquid BF_3OEt_2 (δ = 0 ppm) or to an acidic aqueous solution of $Al(NO_3)_3$ (1M). The spectra were simulated with the DMFIT program [8] which has been developed specifically for solid state NMR experiments, including simulation of quadrupolar shapes [9].

RESULTS AND DISCUSSION

EXAFS at the L_{III}-Nd Edge Spectroscopy

Five glasses were analyzed by EXAFS : Nd2.5, Nd5, Nd10, Nd16 (= Glass A) and Nd30. Fourier transforms of the EXAFS signals (Fig. 1) display a steady decrease of intensity with increasing neodymium amount in glass. According to the fits results (Table I), neodymium always appears surrounded by 8 ± 1 oxygen atoms at a mean distance of 2.46 ± 0.03 Å. Moreover, approximately 3.5 silicon or sodium take place around neodymium ions at about 3.98 ± 0.03 Å. Nevertheless, although boron is not distinguishable by EXAFS, it is very probable, according to the Bray's model [10] for the SiO_2 – B_2O_3 – Na_2O system, to find boron in the vicinity of neodymium in our glasses.

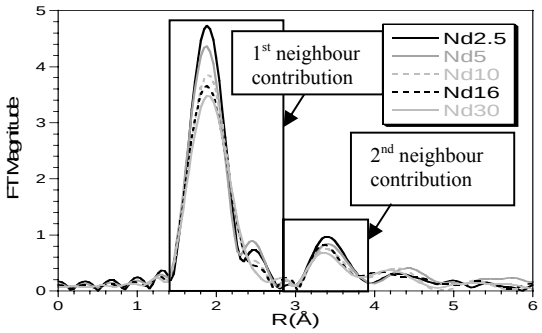

Fig. 1. Fourier transforms of Nd L_{III}-edge EXAFS spectra of glasses containing 2.5, 5, 10, 16 and 30 wt. % Nd_2O_3 (T=77 K).

TABLE I. Quantitative results of the EXAFS analysis of the Ndx glasses with N_i, the number of neighbours, σ_i, the Debye-Waller factor and R_i, the distance (Nd-neighbours).

		Sample number				
		Nd2.5	*Nd5*	*Nd10*	*Nd16*	*Nd30*
Nd–O	N	**8.1**	**8.5**	**7.7**	**8.0**	**7.8**
	R (Å)	**2.44**	**2.45**	**2.47**	**2.46**	**2.48**
	σ^2 (Å^2)	0.020	0.022	0.020	0.021	0.021
	C_3 (Å^3) *10^{-4}	12	14	16	13	17
	C_4 (Å^4) *10^{-5}	41	40	28	29	29
Nd-Si/Na	**N**	**3.5**	**3.5**	**3.5**	**3.5**	**3.5**
	R (Å)	**3.98**	**3.98**	**3.99**	**3.98**	**3.99**
	σ^2 (Å^2)	0.011	0.013	0.014	0.013	0.014

Global quality of fit of 99.7 %

Otherwise, fit tests performed for all glasses with neodymium ions as second neighbours display aberrant fit parameters values (Debye-Waller factor σ > 0.30 Å and quality of fit < 65 %). That means that no phenomena of Nd-Nd clustering at less than 4 Å were detected in these glasses by

EXAFS, even for high neodymium contents. In our glasses, only a significant increase of the static disorder in glass is observed with increasing neodymium concentration (represented by σ^2 (Debye-Waller factor), C_3 and C_4 cumulants), responsible for the decrease of intensity observed on the Fourier transforms.

Optical Absorption Spectroscopy

Optical transmission measurements were performed at T ≈ 10 K. At this temperature, only the first of the five Stark levels of the $^4I_{9/2}$ ground state of neodymium is populated. Among all the electronic transitions of Nd^{3+} ion, two ones are of particular importance for the present investigation. Firstly, the transition between the $^4I_{9/2}$ ground state and the $^2P_{1/2}$ excited state (around 23 225 cm^{-1}, Fig. 2 (a)) brings information on the variety of sites occupied by Nd^{3+} ions in the glass and on the degree of covalency of the bonding (Nd-O). Secondly, the transition between the $^4I_{9/2}$ state and the $^2G_{7/2}$, $^4G_{5/2}$ states (around 17 300 cm^{-1}, Fig. 2 (b)), called hypersensitive, owns shapes strongly affected by changes in the environment around Nd^{3+} ion.

In our glasses, peaks profiles (inhomogeneous half-width and position in energy) of the $^4I_{9/2} \rightarrow {}^2P_{1/2}$ transition of Nd^{3+} (Fig. 2 (a)) do not display any evolution with neodymium concentration in glass. Peaks maxima are all centred at 23 226 cm^{-1} and bands shapes were fitted with one Gaussian getting a constant half-width of 120 cm^{-1}. According to these results, it can be put forward that the (Nd-O) bonding and also the nature of the Nd-surroundings must not show strong evolutions with neodymium content. However, the hypersensitive $^4I_{9/2} \rightarrow {}^2G_{7/2}$, $^4G_{5/2}$ transition (h.s.t.) shape (centred at 17 120 cm^{-1} and 17 460 cm^{-1}) presents slight evolutions with neodymium concentration (Fig. 2 (b)). Indeed, shoulders present at the lowest energy side, strongly emphasized at low neodymium concentrations, become progressively less apparent as $[Nd_2O_3]$ increases, simultaneously occurring with a band broadening. This can either be due to an increase of the Nd-sites distribution and also an increase of the static disorder as neodymium content increases in glass (also shown by EXAFS), or due to an increase of the mean field strength Z/a^2 (Z is the cation valence and a the sum of the cation and oxygen radius, field strength is composed by Na^+, Ca^{2+} and Nd^{3+} contributions). Indeed, according to Dymnikov et al [11], with increasing Z/a^2, the h.s.t. become less resolved and shoulders disappear (for both silicate and borate glasses).

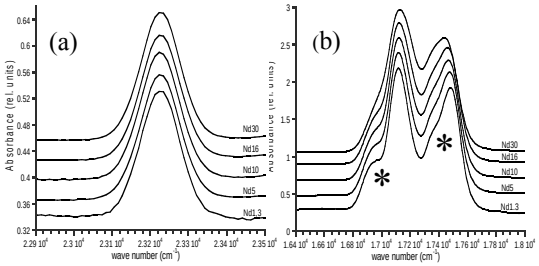

Fig. 2. $^4I_{9/2} \rightarrow {}^2P_{1/2}$ (a) and $^4I_{9/2} \rightarrow {}^2G_{7/2}$, $^4G_{5/2}$ (b) transitions of Nd^{3+} for Ndx glasses at T ≈ 10 K (1.3, 5, 10, 16 and 30 wt. % Nd_2O_3). * indicates shoulders on the band. (The intensities of the peak maxima were normalised to the same arbitrary value).

^{11}B and ^{27}Al MAS-NMR

MAS-NMR studies were realized on glasses prepared with lanthanum instead of neodymium. Indeed, using Nd^{3+} (paramagnetic ion) involves broadened NMR signal shapes due to the dipolar interaction between its electronic spin and the nuclear spin of the studied nuclei.

^{11}B MAS-NMR

Earlier ^{11}B MAS-NMR studies realized on borosilicate minerals and glasses [12-15] have shown that tetrahedral BO_4 and trigonal BO_3 sites exhibit distinct chemical ranges. By integration of the area of these two signals, relative intensities of the two types of sites can be determined (Table II). In these glasses, the BO_3 units proportion, at a fixed BO_4 one, strongly increases as neodymium concentration increases (Fig. 3).

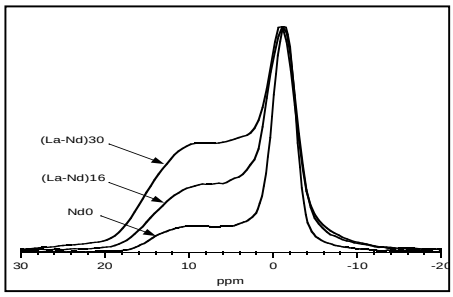

Fig. 3. ^{11}B MAS-NMR signals of glasses containing 0, 16 and 30 wt. % of RE_2O_3. Intensities were normalised to the same arbitrary intensity of the BO_4 shape.

TABLE II. Proportion of BO_3 and BO_4 units in glasses containing 0, 16 and 30 wt. % of RE_2O_3 (RE = Rare Earth)

Sample number	% BO_3 units	% BO_4 units
RE 0	42	58
RE 16	62	38
RE 30	80	20

^{27}Al MAS-NMR

^{27}Al MAS-NMR study allows to determine the different coordination states of the Al^{3+} ions in glasses (Al(IV) around 60 ppm, Al(V) between 25 and 40 ppm or Al(VI) between -15 and 20 ppm). In Ndx glasses, chemical shifts and band shapes do not display any evolution with neodymium content in the glass. At a constant chemical shift of ~ 57 ppm, aluminium ions seem only to be present in four coordination number (Al(IV) units) in all glasses. In oxide glasses, aluminium ions thus form $[AlO_4]^-$ entities [16-18].

Raman Spectroscopy

Raman spectroscopy of oxide glasses is interesting especially in the high-frequency envelope [800 – 1250 cm^{-1}], in which T-O stretch frequencies (with T = Si, Al) occur. As increasing neodymium content in glass, a shift of the SiO_4 Q^n units to the lower frequencies is observed (Fig. 4). According to previous investigations [19-20], this shift could probably be due to the creation of Q^3(Nd) and Q^2(Nd) units, arising at lower frequencies than the corresponding Q^3(Na) and Q^2(Na).

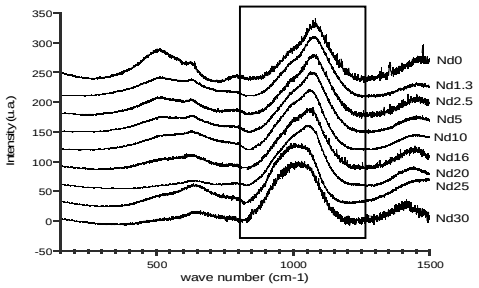

Fig. 4. Raman spectra of Ndx glasses.

CONCLUSIONS

In all Ndx glasses, neodymium appears surrounded by 8 oxygen atoms and ~ 3.5 second neighbors Si / Na / B, with no significant evolutions in the Nd-neighbouring. Only an increase in the Nd-sites distribution is observed along with neodymium content. No Nd-clustering occurs at less than 4 Å. According to all these results, it appears that neodymium probably imposes its environment to the glass.

REFERENCES

1. T. F. Meaker, D. K. Peeler, J. C. Marra, J. M. Pareizs and W. G. Ramsey, *Mat. Res. Soc. Symp. Proc.*, **465,** 1281 (1997).
2. G. Leturcq, G. Berger, T. Advocat and E. Vernaz, *Chemical Geology*, **160**, 39 (1999).
3. A. Michalowicz, EXAFS pour le MAC, in « Logiciels pour la Chimie », Ed. Société Française de Chimie, Paris, p. 102 (1991).
4. A. Michalowicz, *J. Phys. IV, France* **7,** C2-235 (1997).
5. M. Newville, *J. Synchrotron Rad.*, **8,** 96 (2001).
6. G. Dalba, P. Fornasini, F. Rocca, *Phys. Rev. B*, **47** (14), 8502 (1993).
7. P. Fornasini, Nuclear *Instruments and Methods in Physics Research B*, 70 (1995).
8. D. Massiot, F. Fayon, M. Capron, I. King, S. Le Calvé, B. Alonso, J.-O. Durand, B. Bujoli, Z. Gan, G. Hoatson, *Magn. Reson. Chem.*, **40**, 70 (2002).
9. A. P. M. Kentgens, *Geoderma*, **80,** 271 (1997).
10. W. J. Dell, P. J. Bray, S. Z. Xiao, *J. Non-Cryst. Solids*, **58**, 1 (1983).
11. A. A. Dymnikov and A.K.Przhevuskii, *J. Non-Cryst. Solids*, **215**, 83 (1997).
12. W. J. Dell, P. J. Bray, S. Z. Xiao, *J. Non-Cryst. Solids*, **58**, 1 (1983).
13. A. H. Silver, P. J. Bray, *J. Chem. Phys*., **29**, 984 (1985).
14. W. Müller-Warmuth, H. Eckert, *Phys. Rep*., **88,** 91 (1982).
15. G. L. Turner, K. A. Smith, R. J. Kirkpatrick, E. Oldfield, J. Magn. Res., **67**, 544 (1986).
16. G. Engelhardt, D. Michel, High resolution solid-state NMR in silicates and zeolites, Wiley, New-York (1987).
17. M. E. Smith, *Appl. Magn. Reson*., **4**, 1 (1993).
18. J. F. Stebbins, *Handbook of physical constants*, **2**, 303 (1995).
19. H. Li, Y. Su, L. Li, D. M. Strachan, *J. Non-Cryst. Solids*, **292**, 167 (2001).
20. Z. N. Utegulov, ML. A. Eastman, S. Prabakar, K. T. Mueller, A. Y. Hamad, J. P. Wicksted, G. S. Dixon, *J. Non-Cryst. Solids*, **315**, 43 (2003).